PAD4 silencing inhibits inflammation whilst promoting trophoblast cell invasion and migration by inactivating the NEMO/NF-κB pathway

MIN ZENG, MINJUAN XU, XIAFANG LI, JUNYING LI and YUANYUAN LIU

Department of Obstetrics, Ganzhou People's Hospital, Ganzhou, Jiangxi 341001, P.R. China

Received May 18, 2021; Accepted September 29, 2021

DOI: 10.3892/etm.2022.11505

Abstract. Preeclampsia (PE), presenting with onset hypertension and proteinuria, is a pregnancy-specific disorder that can result in maternal and fetal morbidity and mortality. Insufficient trophoblast invasion and migration has been considered to be an important cause of this disease. The present study aimed to investigate the role of peptidyl arginine deiminase 4 (PAD4), whose knockdown has been previously indicated to reduce inflammation and susceptibility to pregnancy loss in mice, in the development of PE *in vitro*. Lipopolysaccharide (LPS) was used to treat a human trophoblast cell line (HTR8/SVneo). After PAD4 silencing via transfection with short hairpin RNA against PAD4, the concentrations of inflammatory factors IL-6, IL-12 and monocyte chemoattractant protein (MCP)-1 were measured using ELISA. Cell viability was also measured using Cell Counting Kit-8 assay. HTR8/SVneo cell invasion and migration were detected using Transwell and wound healing assays, respectively. Western blotting was used to measure the expression of citrullinated NF-κB essential modulator (NEMO) and nuclear NF-κB p65 protein levels. TNF-α was applied for evaluating the potential regulatory effects of PAD4 on NF-κB in LPS-stimulated HTR8/SVneo cells. LPS increased the levels of IL-6, IL-12 and MCP-1 and reduced the migration and invasion of HTR8/SVneo cells. PAD4-knockdown was found to markedly reduce the levels of IL-6, IL-12 and MCP-1 secretion. HTR8/SVneo cell invasion and migration was also significantly elevated after PAD4 silencing following LPS exposure. In addition, LPS stimulation notably upregulated the protein levels of citrullinated NEMO and nuclear NF-κB p65, which was restored by PAD4 knockdown. Furthermore, TNF-α treatment partially counteracted the effects of PAD4 knockdown on the secretion of IL-6, MCP-1 and IL-12, which are markers of inflammation, and invasion and migration in LPS-induced HTR8/SVneo cells. To conclude, these results suggest that PAD4 silencing can suppress inflammation whilst promoting invasion and migration by trophoblast cells through inhibiting the NEMO/NF-κB pathway. These findings furthered the understanding in the complex molecular mechanism that can trigger PE and provide a promising target for the treatment of this disease.

Correspondence to: Dr Min Zeng, Department of Obstetrics, Ganzhou People's Hospital, 16 Meiguan Avenue, Ganzhou, Jiangxi 341001, P.R. China
E-mail: zengmin07@126.com

Key words: preeclampsia, peptidyl arginine deiminase 4, trophoblast cells, inflammation, invasion

Introduction

Preeclampsia (PE) is a pregnancy-specific condition that affects ~10% pregnancies worldwide and is one of the leading causes of maternal and neonatal morbidity and mortality (1,2). Trophoblast cells form the external tissues of embryos and serve an important role in embryo development (3,4). Insufficient invasion of cytotrophoblasts (CTBs) into the uterine artery has been suggested to be an important factor in PE pathogenesis (3,4). Despite improvements in perinatal care, PE remains to be a serious clinical problem. Therefore, it is of clinical and scientific significance to identify novel therapeutic targets associated with this disease.

Peptidyl arginine deiminase 4 (PAD4) is an enzyme that mediates the citrullination (post-translational deamination) of arginine residues to citrullines, which reverses chromatin condensation (5,6). A previous study has proposed that PAD4 knockdown can reduce inflammation and susceptibility to pregnancy loss in mice (7). In addition, it has been reported that PAD4 could promote the nuclear translocation of NF-κB and activate NF-κB signaling through NF-κB essential modulator (NEMO) citrullination, which contributed to inflammation and transformed the expression of several genes involved in the pathogenesis of PE (8-10). The *NEMO* gene, which induces the activation of NF-κB, is located on the sex chromosome Xq28 and has been reported to be notably decreased in pregnancies complicated by PE (11). Upregulated NEMO expression in the maternal and fetal blood has been reported to be closely associated with the development of PE (12). Furthermore, total NEMO (1A, 1B and 1C transcripts) in maternal blood and placentas of the PE subgroup were previously found to be significantly increased compared with the controls (13). Therefore, this suggested that PAD4 knockdown can reduce the inflammation by regulating the NEMO/NF-κB signaling pathway, thereby inhibiting the progression of PE.

In the present study, lipopolysaccharide (LPS) was used to treat human trophoblast cells (HTR8/SVneo) to simulate the PE model *in vitro* to evaluate the role of PAD4 in the inflammation, invasion and migration of HTR8/SVneo cells and investigate its potential regulatory effects on the NEMO/NF-κB signaling pathway (14). These findings might provide a theoretical and experimental basis for exploring a novel target for the treatment of PE.

Materials and methods

Cell culture. The human trophoblast cell line HTR8/SVneo was obtained from American Type Culture Collection. HTR8/SVneo cells were previously developed by Graham *et al* (15). It was generated using freshly isolated extravillous CTB from first trimester placenta and transfected with a plasmid containing the simian virus 40 large T antigen (SV40). A previous study demonstrated that this cell line contains two populations, one of epithelial and the other of mesenchymal origin (16). In the present study, HTR-8/SVneo cells were cultured in RPMI-1640 medium (Gibco; Thermo Fisher Scientific, Inc.) containing 10% fetal bovine serum (FBS; Gibco; Thermo Fisher Scientific, Inc.). The incubator was set as having 5% CO_2 with a humidified atmosphere at 37˚C. To determine the effects of LPS on HTR-8/SVneo cells, LPS (200 ng/ml; Sigma-Aldrich; Merck KGaA) was added to the culture medium for 48 h at 37˚C, which was according to the previous study (17).

Cell transfection. The pLVX lentiviral plasmid containing the short hairpin RNA (shRNA) against PAD4 (shPAD4#1 or shPAD4#2) or a scrambled shRNA (shNC) were synthesized by Shanghai GenePharma Co., Ltd. The transfection (50 ng plasmid) was done using Lipofectamine 3000 (Invitrogen; Thermo Fisher Scientific, Inc.) at 37˚C for 48 h, in accordance with the manufacturer's protocols. Transfection efficiency was evaluated using reverse transcription-quantitative PCR (RT-qPCR) following 48 h of transfection. After 48 h transfection, HTR8/SVneo cells were also harvested for further experiments. The targeting sequences were as follows: shPAD4#1, 5'-GGTGACCCTGACGATGAAAGT-3'; shPAD4#2, 5'-GCAGCTCTTCAAGCTCAAAGA-3'; and shNC, 5'-TTCTCCGAACGTGTCACGT-3'.

Cell viability assay. For assessment of cell viability, cells were seeded into 96-well plates and analyzed using Cell Counting Kit-8 (CCK-8; Beijing Solarbio Science & Technology Co., Ltd.). Briefly, after PAD4 knockdown and treatment with LPS (0, 100, 500, 1,000 and 1,500 ng/ml) for 12 h and TNF-α for 4 h, 10 μl CCK-8 working solution was added to each well, followed by incubation with normal cell culture medium for 2 h at 37˚C. Optical density in each well was then evaluated at the 450 nm using a microplate reader (Bio-Rad Laboratories, Inc.).

Measurement of inflammatory factors. The contents of inflammatory cytokines IL-6 (cat. no. F01440), IL-12 (cat. no. F01380) and monocyte chemoattractant protein (MCP)-1 (cat. no. F01700) in the culture media were measured using ELISA according to the manufacturer's protocol (Shanghai Xitang Biotechnology Co., Ltd.). The optical density values were then read on a plate reader (BioTek Instruments, Inc.).

Transwell assay. Transwell assay was performed using 24-well culture plates with 8-mm pore-size Falcon Transwell inserts (BD Biosciences). HTR8/SVneo cells ($1x10^5$ cell/well) were suspended in 200 μl serum-free RPMI 1640 and seeded into the upper chamber of the Matrigel-coated Transwell insert for 8 h at 37˚C. RPMI 1640 medium containing 10% FBS was placed into the lower chamber. After 24 h of incubation at 37˚C, cells were fixed with 4% paraformaldehyde (Sigma-Aldrich; Merck KGaA) for 30 min at room temperature and then stained with 0.1% crystal violet (Sigma-Aldrich; Merck KGaA) for 20 min at room temperature. The stained cells were photographed under an inverted light microscope (magnification, x100; Olympus Corporation). Image J software v1.8.0 (National Institutes of Health) was used to calculate the numbers of cells invaded in ≥5 random images.

Wound healing assay. For wound healing assay, HTR8/SVneo cells were seeded into six-well plates at a density of $5x10^5$ cells/well and cultured to 90% confluence. A 200-μl sterile pipette gun was used to create a wound on the cell surface. The cells were then cultured in serum-free RPMI 1640 medium and cell migration was measured at 0 and 48 h and 37˚C by detecting the average distance of cells migrating into the wound as observed using inverted light microscopy (magnification, x100; Olympus Corporation). Relative cell migration rate=(scratch width at 0 h-scratch width after culture)/scratch width at 0 h.

RT-qPCR analysis. Total RNA was extracted from HTR8/SVneo cells using TRIzol reagent (Invitrogen; Thermo Fisher Scientific, Inc.) in accordance with the manufacturer's protocol. Complementary DNA (cDNA) was synthesized using the PrimeScript™ RT Reagent Kit (Takara Bio, Inc.). The temperature protocol was as follows: 16˚C for 30 min, 42˚C for 30 min and 85˚C for 5 min, followed by storage at 4˚C. qPCR was then performed using 2 μg cDNA as the template and Power SYBR® Green Master Mix (Applied Biosystems; Thermo Fisher Scientific, Inc.) on the ABI 7500 PCR system (Applied Biosystems; Thermo Fisher Scientific, Inc.) with the following thermocycling conditions: 30 sec at 95˚C for 1 cycle; 3 sec at 95˚C, 30 sec at 60˚C and 30 sec at 72˚C for 40 cycles; and 5 min at 72˚C for 1 cycle. The following primer sequences were used in the present study: PAD4 forward, 5'-CCCAAACAGGGGGTATCAGT-3' and reverse, 5'-CCACGGACAGCCAGTCAGAA-3' and GAPDH forward, 5'-TGTGGGCATCAATGGATTTGG-3' and reverse, 5'-ACACCATGTATTCCGGGTCAAT-3'. GAPDH was used as the internal reference gene. Relative gene expression levels were calculated using the $2^{-\Delta\Delta Cq}$ method (18).

Western blot analysis. Total HTR-8/SVneo cell protein extracts were obtained using RIPA lysis buffer (Beyotime Institute of Biotechnology). Nuclear and cytosolic proteins were extracted using the Nucleoprotein and Cytoplasmic Protein Extraction Kit obtained from Nanjing KeyGen Biotech Co., Ltd. Concentrations of proteins were quantified

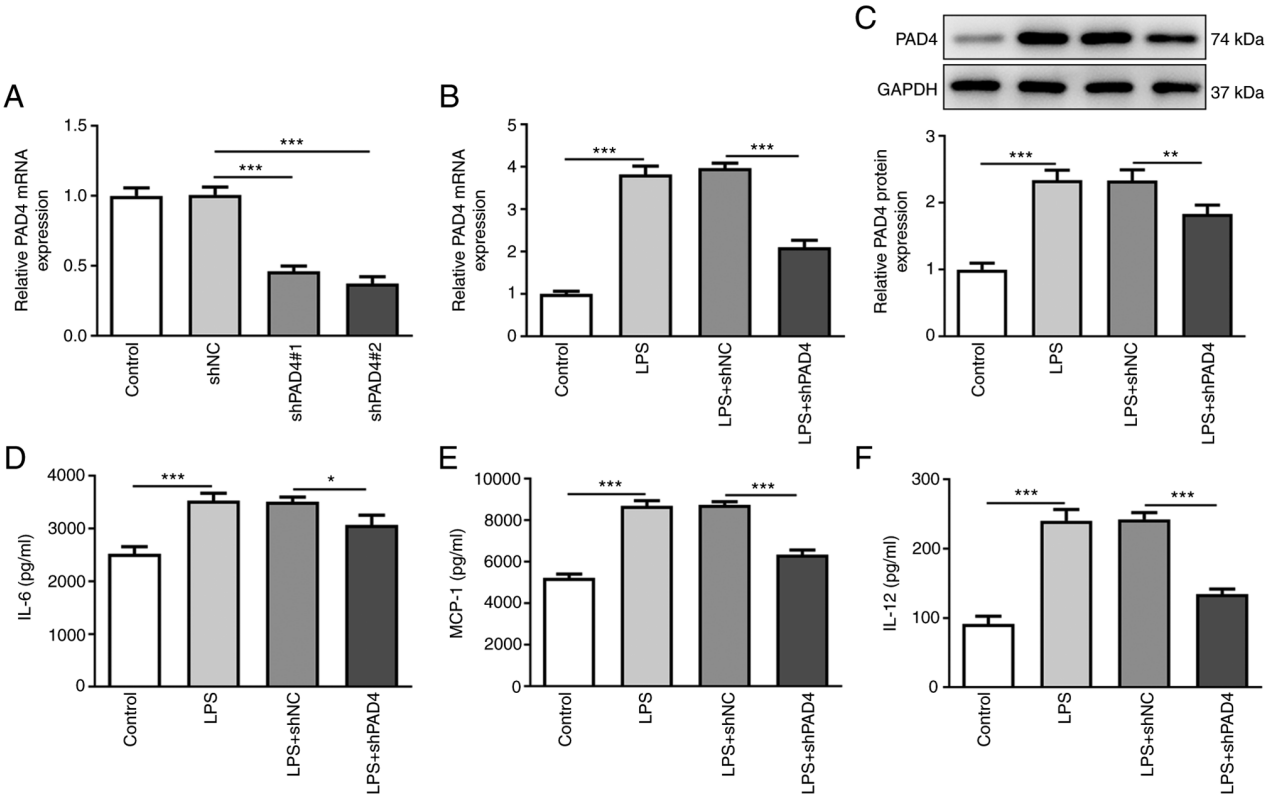

Figure 1. PAD4 knockdown alleviates the inflammatory response in LPS-treated HTR8/SVneo cells. (A) PAD4 expression was measured by RT-qPCR after transfection with shNC, shPAD4#1 or shPAD4#2 in HTR8/SVneo cells. The expression of (B) PAD4 mRNA and (C) protein in LPS-stimulated HTR8/SVneo cells transfected with PAD4 shPAD4 was measured with RT-qPCR and western blot analysis, respectively. The concentrations of inflammatory factors including (D) IL-6, (E) MCP-1 and (F) IL-12 were examined using ELISA kits. *P<0.05, **P<0.01 and ***P<0.001. PAD4, peptidyl arginine deiminase 4; LPS, lipopolysaccharide; RT-qPCR, reverse transcription-quantitative PCR; sh, short hairpin; NC, negative control; MCP-1, monocyte chemoattractant protein-1.

using a BCA kit (Beyotime Institute of Biotechnology). Equal amounts of each protein sample (40 μg) were added per lane and separated by electrophoresis in 10% SDS-PAGE and transferred onto PVDF membranes. Possible non-specific binding was blocked by 5% skimmed milk for 1 h at room temperature and then incubated overnight at 4˚C with specific primary antibodies: Anti-PAD4 (cat. no. ab214810; 1:1,000; Abcam), anti-NEMO (cat. no. 2685S; 1:1,000; Cell Signaling Technology, Inc.), anti-NF-κB p65 (cat. no. 8242T; 1:1,000; Cell Signaling Technology, Inc.), anti-Histone H3 (cat. no. 4499T; 1:1,000; Cell Signaling Technology, Inc.) and anti-GAPDH (cat. no. 5174T; 1:1,000; Cell Signaling Technology, Inc.). The next day, goat anti-rabbit HRP-conjugated secondary antibodies (cat. no. 31460; 1:10,000; Thermo Fisher Scientific, Inc.) were added to the membranes and incubated for 1 h at room temperature. Protein bands were scanned and visualized using an enhanced chemiluminescence detection system (Life Technologies; Thermo Fisher Scientific, Inc.). The relative intensity of each band was quantified using Image J software v1.8.0 (National Institutes of Health). The protein expression was normalized to either GAPDH or Histone H3 levels.

Immunoprecipitation. HTR-8/SVneo cells were lysed using lysis buffer for immunoprecipitation (cat. no. 26146; Pierce; Thermo Fisher Scientific, Inc.). Citrulline was immunoprecipitated from 50 μg samples using an anti-citrulline antibody (cat. no. ab240908; Abcam) and incubated for 1 h at 4˚C. This antibody-citrulline protein immunocomplex was captured from the solution using 50 μg Protein A/G Plus agarose beads (Santa Cruz Biotechnology, Inc.) and incubated overnight at 4˚C. Samples were then centrifuged at 1,000 x g for 1 min at 4˚C and the pellet was washed with PBS for three times followed by boiling in Laemmli buffer (Cell Signaling Technology, Inc.) for 5 min at 100˚C. Total lysates and immunoprecipitated samples were then subjected to western blotting analysis.

Statistical analysis. GraphPad Prism software (version 8.0; GraphPad Software, Inc.) was applied for data analysis. Data were expressed as the mean ± standard deviation from three independent experiments. Comparison between two independent groups was conducted using unpaired Student's t test. Comparisons among multiple groups were analyzed using one-way ANOVA followed by Tukey's post hoc test. P<0.05 was considered to indicate a statistically significant difference.

Results

PAD4 silencing attenuates the inflammatory response by LPS-induced HTR8/SVneo cells. The expression of PAD4 was measured after transfection with shPAD4#1 or shPAD4#2. Significantly decreased PAD4 expression was observed in HTR8/SVneo cells transfected with shPAD4#1 or shPAD4#2 compared with that in the shNC group (Fig. 1A). shPAD4#2 was selected for subsequently experiments due to the lower

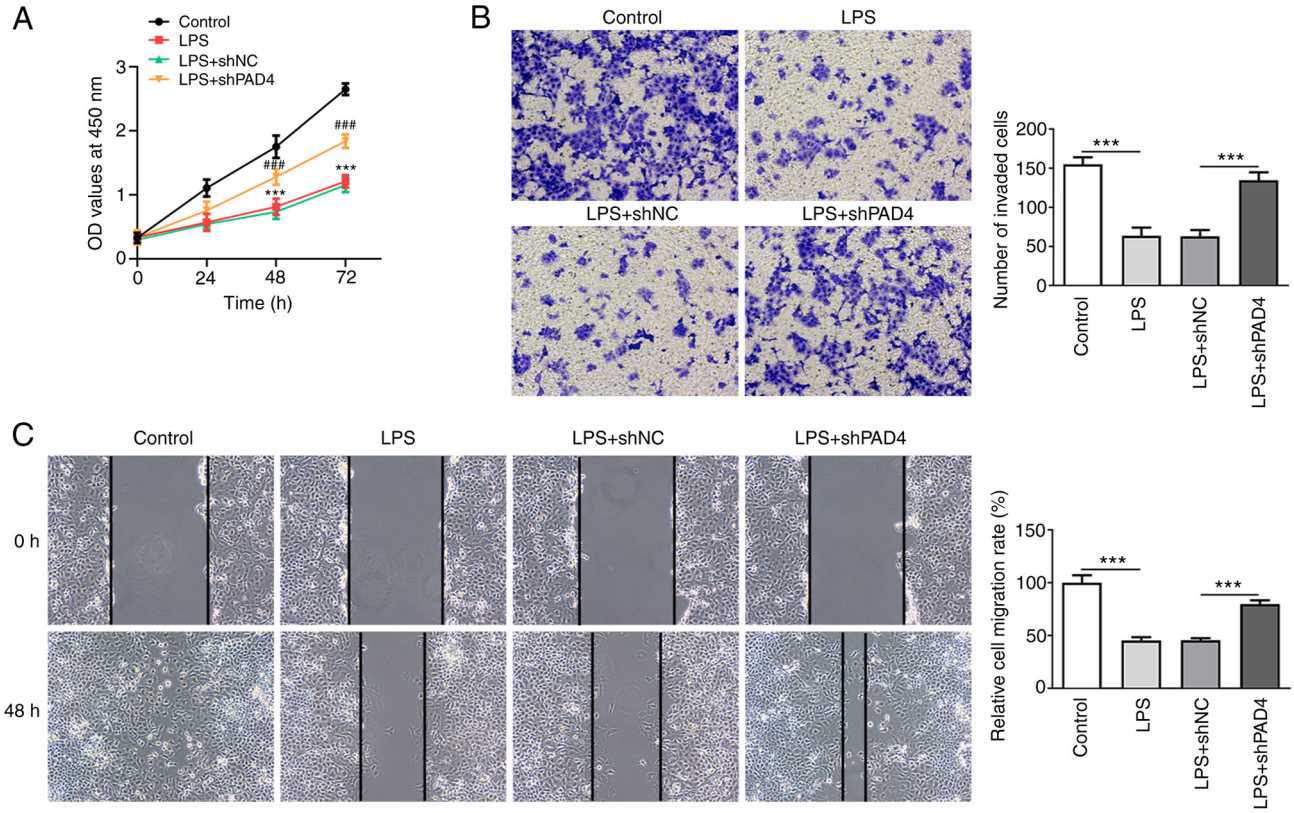

Figure 2. PAD4 knockdown promotes the invasion and migration of HTR8/SVneo cells following exposure to LPS. (A) Cell viability was evaluated using Cell Counting Kit-8 assay. ***P<0.001 vs. Control and ###P<0.001 vs. LPS + shNC. (B) Cell invasion was measured by using Transwell assay. (C) Cell migration was assessed using wound healing assay. ***P<0.001. PAD4, peptidyl arginine deiminase 4; LPS, lipopolysaccharide; OD, optical density; sh, short hairpin; NC, negative control.

PAD4 expression levels induced. To evaluate the role of PAD4 following LPS-induced inflammation in HTR8/SVneo cells, PAD4 expression was silenced by transfection with shPAD4#2. As shown in Fig. 1B and C, LPS stimulation led to a significant increase in PAD4 mRNA and protein expression compared with that in the control group, which was significantly reversed by PAD4 knockdown. Subsequently, the levels of inflammatory factors were measured using ELISA. The levels of IL-6, MCP-1 and IL-12 were significantly elevated after HTR8/SVneo cells exposed to LPS (Fig. 1D-F). By contrast, PAD4 knockdown partially reversed the promoting effects of LPS on the secretion of IL-6, MCP-1 and IL-12 (Fig. 1D-F). These findings suggest that PAD4 knockdown can attenuate the inflammatory response in LPS-induced HTR8/SVneocells.

PAD4 silencing promotes the invasion and migration of HTR8/SVneo cells following exposure to LPS. Cell viability was measured using CCK-8 assay. A significantly deceased HTR8/SVneo cell viability was observed in the LPS-induced group compared with that in the control group, which was significantly reversed after transfection with shPAD4#2 (Fig. 2A). LPS stimulation also significantly inhibited the invasive ability of HTR8/SVneo cells compared with that in the control group (Fig. 2B). By contrast, PAD4 knockdown significantly increased cell invasion compared with that in the LPS + shNC group (Fig. 2B). In addition, LPS significantly suppressed the migration of HTR8/SVneo cells, though PAD4 silencing partially but significantly reversed this inhibitory effect on the migration of HTR8/SVneo cells after LPS challenge (Fig. 2C). These results suggest that silencing of PAD4 expression can promote the invasion and migration of HTR8/SVneo cells after treatment with LPS.

Knocking down PAD4 expression inhibits NEMO citrullination and reduces NF-κB nuclear translocation in LPS-treated HTR8/SVneo cells. To explore the potential mechanism of PAD4 in the progression of PE, the expression of proteins in the NEMO/NF-κB signaling pathway was measured by western blot analysis. Compared with that in the control group, LPS treatment significantly upregulated the expression of citrullinated NEMO whilst significantly downregulating total NEMO expression, which was significantly reversed by PAD4 silencing (Fig. 3A). In addition, significantly increased nuclear NF-κB p65 protein levels and significantly decreased cytoplasmic NF-κB p65 protein levels were noted in the LPS group compared with those in the control group, which was also significantly reversed by PAD4 knockdown (Fig. 3B). These observations suggest that knocking down PAD4 expression can suppress NEMO citrullination and decrease nuclear NF-κB translocation in LPS-induced HTR8/SVneo cells.

TNF-α reverses the effects of PAD4 silencing on inflammation, invasion and migration in LPS-induced HTR8/SVneo cells. TNF-α was subsequently used to treat HTR8/SVneo cells to activate NF-κB signaling to evaluate the effects of PAD4 silencing on inflammation, invasion and migration was

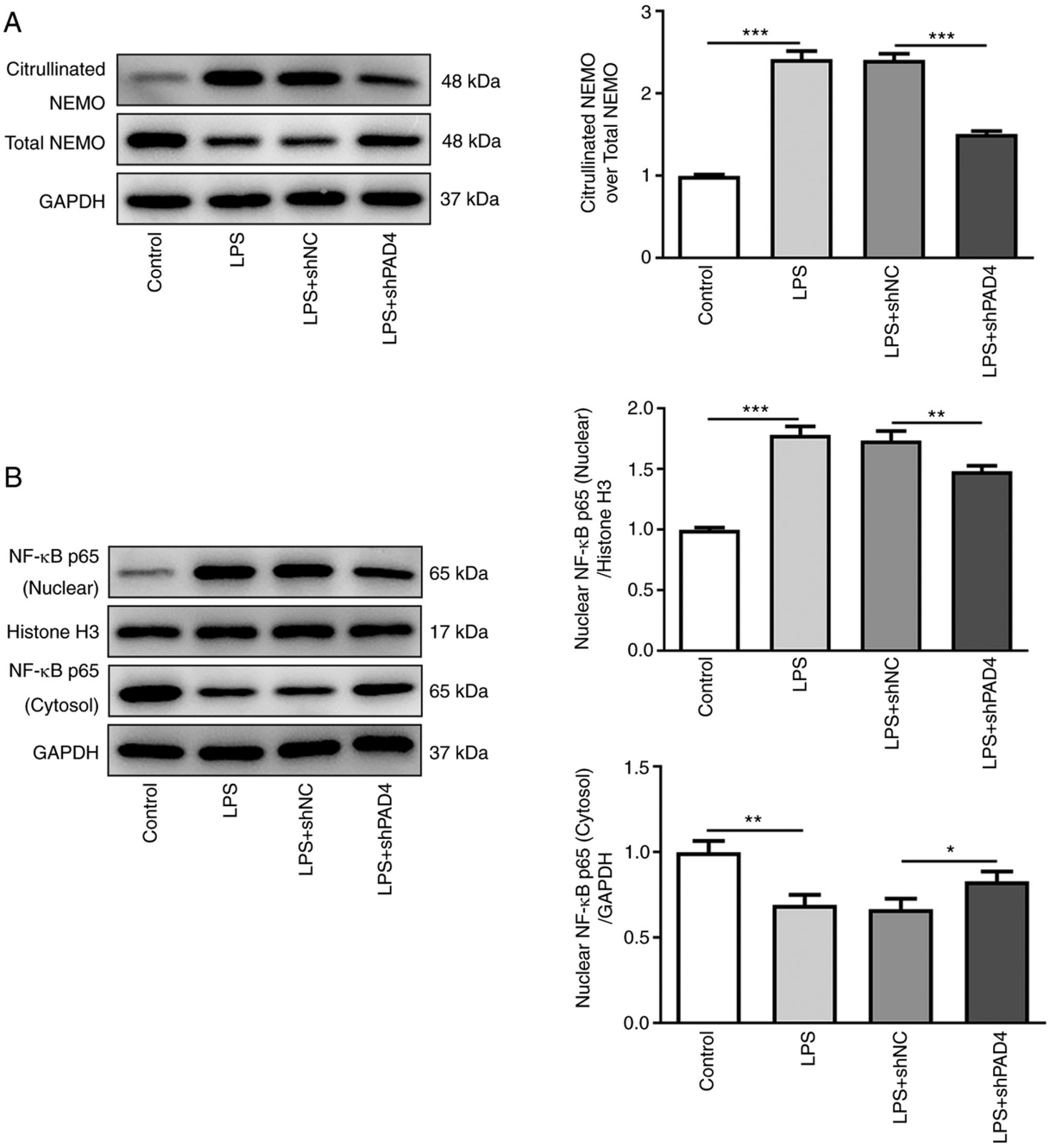

Figure 3. PAD4 knockdown inhibits NEMO citrullination whilst reducing nuclear NF-κB translocation in LPS-stimulated HTR8/SVneo cells. (A) The expression of citrullinated NEMO (immunoprecipitated sample) and total NEMO (cell lysate) was measured using western blot analysis. (B) The expression of nuclear NF-κB p65 and cytoplasmic NF-κB p65 was evaluated using western blot analysis. *P<0.05, **P<0.01 and ***P<0.001. PAD4, peptidyl arginine deiminase 4; LPS, lipopolysaccharide; NEMO, NF-κB essential modulator; sh, short hairpin; NC, negative control.

mediated by NEMO/NF-κB signaling. TNF-α intervention significantly elevated the level of nuclear NF-κB p65 expression and reduced that of cytoplasmic NF-κB p65 expression compared with that in the untreated LPS + shPAD4 group (Fig. 4A). In addition, it was found that the secretion levels of IL-6, MCP-1 and IL-12 were markedly enhanced after the HTR8/SVneo cells were treated with TNF-α compared with those in the untreated LPS + shPAD4 group (Fig. 4B-D).

Downstream, TNF-α treatment led to significantly increased cell viability compared with that in the untreated LPS + shPAD4 group (Fig. 5A). In addition, the abilities of HTR8/SVneo cell invasion and migration were significantly reduced after treatment with TNF-α, LPS exposure and PAD4 silencing compared with that in the untreated LPS + shPAD4 group (Fig. 5B and C). Collectively, these data suggest that PAD4 silencing inhibits inflammation and promotes the invasion and migration of trophoblast cells by inactivation of the NEMO/NF-κB signaling pathway.

Discussion

PE is a pregnancy-specific syndrome that originates from the placenta with a number of systems involved, including the liver, kidney and cardiovascular systems (19,20). It is

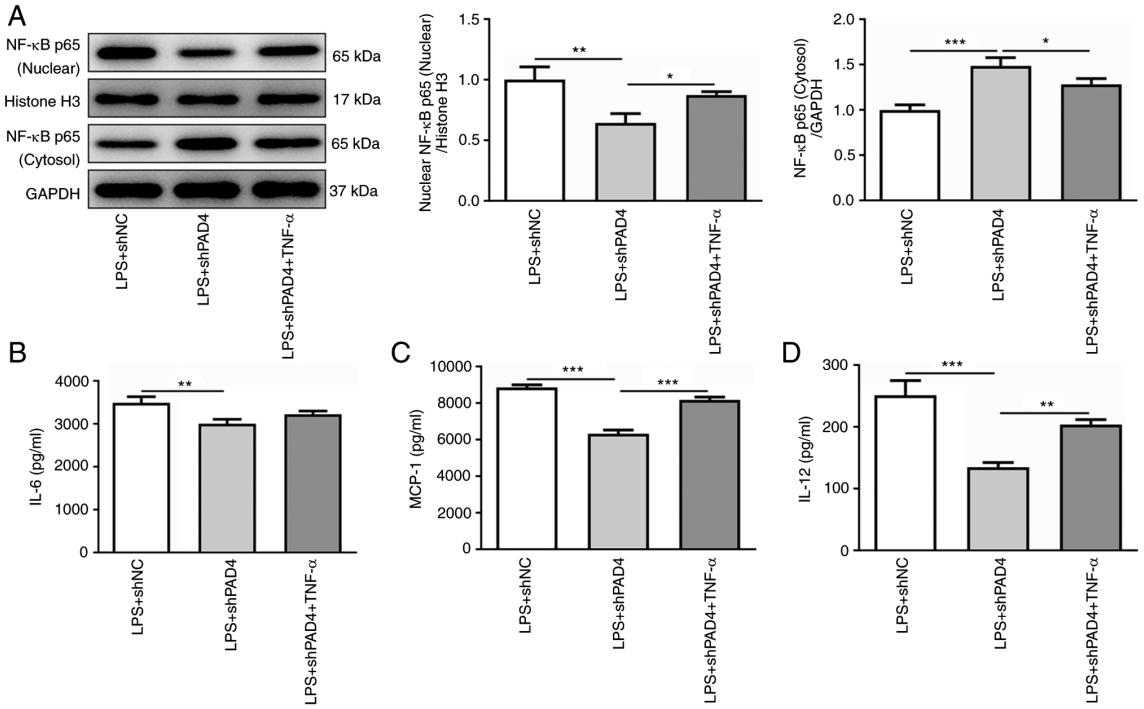

Figure 4. TNF-α reverses the inhibitory effects of PAD4 knockdown on the inflammation of LPS-induced HTR8/SVneo cells. (A) Western blot analysis was performed to measure the expression of nuclear NF-κB p65 and cytoplasmic NF-κB p65 protein after TNF-α treatment. The concentrations of (B) IL-6, (C) MCP-1 and (D) IL-12 were measured using ELISA. *P<0.05, **P<0.01 and ***P<0.001. PAD4, peptidyl arginine deiminase 4; LPS, lipopolysaccharide; sh, short hairpin; NC, negative control; MCP-1, monocyte chemoattractant protein-1.

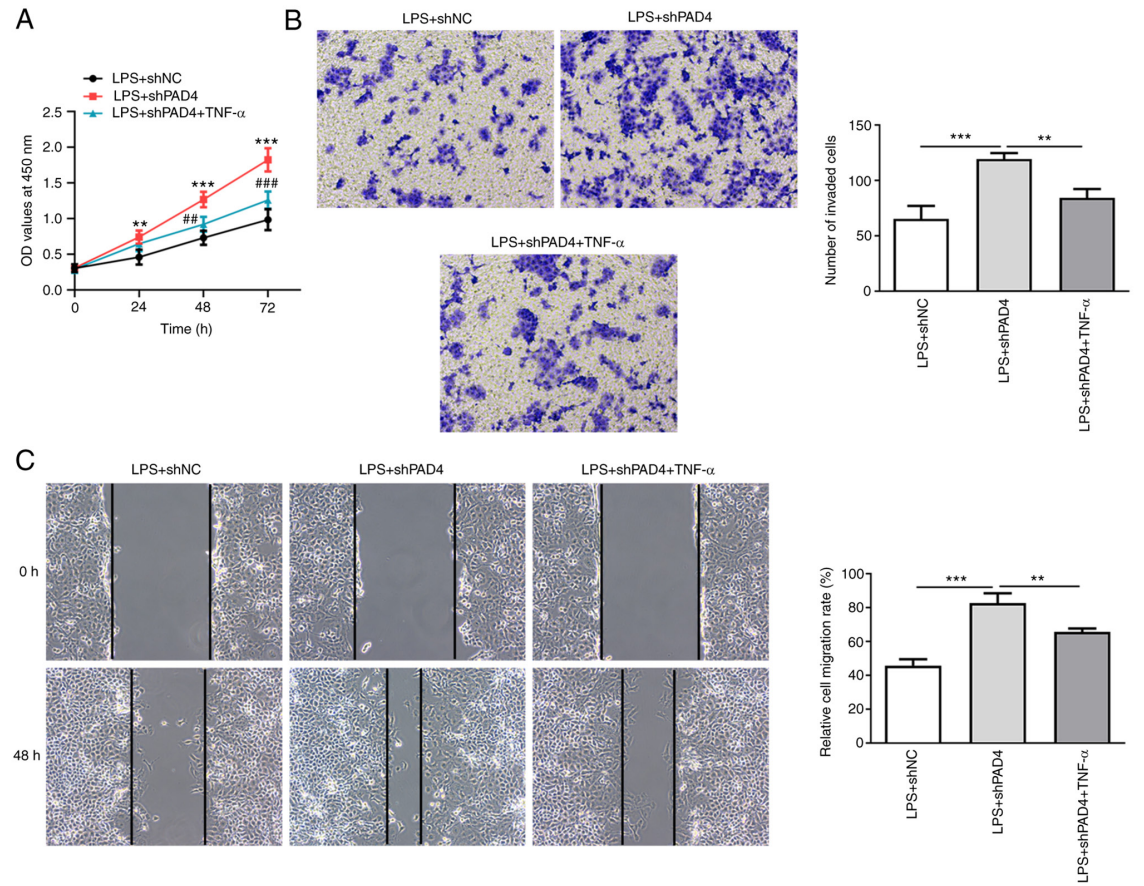

Figure 5. TNF-α alleviates the impact of PAD4 knockdown on the invasion and migration of LPS-induced HTR8/SVneo cells. (A) Cell viability was evaluated using Cell Counting Kit-8 assay. **P<0.01 and ***P<0.001 vs. LPS + shNC; $^{\#\#}$P<0.01 and $^{\#\#\#}$P<0.001 vs. LPS + shPAD4. (B) Cell invasion was measured using Transwell assay. (C) Cell migration was assessed using wound healing assay. **P<0.01 and ***P<0.001. PAD4, peptidyl arginine deiminase 4; LPS, lipopolysaccharide; OD, optical density; sh, short hairpin; NC, negative control.

potentially life-threatening for both mother and baby (21). It is widely accepted that PE is typically caused by insufficient trophoblastic infiltration into the endometrium during embryonic development, leading to severe endothelial malfunction in the uterine placenta (22). The present study demonstrated that PAD4 expression is increased following LPS treatment in HTR8/SVneo cells *in vitro*. Mechanistically, PAD4 silencing could inhibit inflammation whilst promoting invasion and migration of trophoblast cells by inactivating the NEMO/NF-κB signaling pathway.

Previous studies have reported that an altered immune system response and excessive inflammation can contribute to the development of PE (23,24). Inflammatory responses at the utero-placental interface were associated with deficient extravillous trophoblast invasion during placentation in transgenic preeclamptic rat models and patients with PE (18,25). Several *in vitro* studies previously suggested that exposure to inflammatory stimuli can trigger the secretion of proinflammatory cytokines from trophoblast cells, such as IL-6, IL-12 and MCP-1, to mediate PE (26,27). PAD4 is an enzyme that catalyzes the citrullination process and serves a significant role in innate immunity, infection control and autoimmune diseases (5,28). Shelef *et al* (29) suggested that PAD4 contributes to TNF-α-induced inflammatory arthritis. In PAD4-null mice, the renal neutrophil infiltration and inflammation after ischemia-reperfusion injury were markedly alleviated compared with those in wild-type mice (30). In addition, loss of PAD4 function has been reported to reduce inflammation and susceptibility to pregnancy loss in a PAD4 knockout mouse model (7). In the present study, reduced levels of inflammatory factors IL-6, MCP-1 and IL-12 as a result of PAD4 silencing in LPS-induced HTR8/SVneo cells provided further support for the potential role of PAD4 in PE during pregnancy.

During the development of placenta, cytotrophoblast proliferation, invasion and migration are orchestrated steps critical for normal pregnancy (31,32). Efficient trophoblastic infiltration forms the basis for the effective establishment of uteroplacental circulation and is key to successful pregnancy (33). Insufficient invasion and migration of trophoblast cells results in shallow embryo implantation, inadequate placental invasion and abnormal spiral artery remodeling, which are generally regarded to be major mechanisms underlying PE (34). To the best of our knowledge, the present study is the first to explore the effects of PAD4 on the invasion and migration of HTR8/SVneo cells following exposure to LPS, where PAD4 silencing promoted the invasion and migration of HTR8/SVneo cells.

Subsequently, the potential mechanism of PAD4 in the development of PE was investigated in the present study. Consistent with the previous findings (8,9), the results indicate that PAD4 can promote the NF-κB nuclear translocation and activate NF-κB activity through NEMO citrullination. The expression of NEMO was found to be conspicuously higher in the maternal and fetal blood of PE cases compared with that in healthy controls (11). Importantly, the NEMO transcription level in maternal blood of the PE subgroup was significantly increased (12). NEMO is one of the regulatory subunits of the IκB kinase (IκK) complex, which controls activation of NF-κB signaling pathway (35). It has been reported that the NF-κB and TNF-α in the NF-κB pathway are highly expressed in the peripheral blood mononuclear cells of patients with PE, compared with the control group (36). In the present study, PAD4 silencing downregulated the expression of citrullinated NEMO and nuclear NF-κB p65 expression, suggesting that PAD4 may regulate the NEMO/NF-κB pathway in LPS-induced HTR8/SVneo cells. Furthermore, activation of NF-κB signaling by the addition of TNF-α reversed the impact of PAD4 silencing on the inflammation, invasion and migration of HTR8/SVneo cells. The present study is a preliminary study of the role of PAD4 in PE by an LPS-induced HTR8/SVneo cell model. The lack of *in vivo* experiments to investigate the effects of PAD4 on an animal PE model and the experiments for the examination of related signaling pathways that can be regulated by PAD4 are limitations of the present study. Therefore, further comprehensive and in-depth analyses are required to validate the findings of the present study.

Taken together, the present study suggests that PAD4 is highly expressed in LPS-induced HTR8/SVneo cells *in vitro*. Mechanistically, PAD4 silencing inhibited inflammation but promoted the invasion and migration of trophoblasts by inactivating the NEMO/NF-κB signaling pathway. These findings lay a foundation for furthering the understanding in the complex molecular mechanisms underlying PE and provide a promising target for the treatment of this disease.

Acknowledgements

Not applicable.

Funding

No funding was received.

Availability of data and materials

The datasets used and/or analyzed during the current study are available from the corresponding author on reasonable request.

Authors' contributions

MZ, MX and XL searched the literature, designed the experiments and conducted the experiments. JL and YL analyzed and interpreted the data. MZ and MX wrote the manuscript. XL and YL revised the manuscript. MZ and MX confirmed the authenticity of all the raw data. All authors have read and approved the final version of the manuscript.

Ethics approval and consent to participate

Not applicable.

Patient consent for publication

Not applicable.

Competing interests

The authors declare that they have no competing interests.

References

1. Capriglione S, Plotti F, Terranova C, Gulino FA, Di Guardo F, Lopez S, Scaletta G, and Angioli R: Preeclampsia and the challenge of early prediction: Reality or utopia? State of art and critical review of literature. J Matern Fetal Neonatal Med 33: 677-686, 2020.
2. Mazzuca MQ, Li W, Reslan OM, Yu P, Mata KM and Khalil RA: Downregulation of microvascular endothelial type B endothelin receptor is a central vascular mechanism in hypertensive pregnancy. Hypertension 64: 632-643, 2014.
3. Li X, Wu C, Shen Y, Wang K, Tang L, Zhou M, Yang M, Pan T, Liu X and Xu W: Ten-eleven translocation 2 demethylates the MMP9 promoter, and its down-regulation in preeclampsia impairs trophoblast migration and invasion. J Biol Chem 293: 10059-10070, 2018.
4. Xie N, Jia Z and Li L: miR-320a upregulation contributes to the development of preeclampsia by inhibiting the growth and invasion of trophoblast cells by targeting interleukin 4. Mol Med Rep 20: 3256-3264, 2019.
5. Rohrbach AS, Slade DJ, Thompson PR and Mowen KA: Activation of PAD4 in NET formation. Front Immunol 3: 360, 2012.
6. Wang S and Wang Y: Peptidylarginine deiminases in citrullination, gene regulation, health and pathogenesis. Biochim Biophys Acta 1829: 1126-1135, 2013.
7. Erpenbeck L, Chowdhury CS, Zsengellér ZK, Gallant M, Burke SD, Cifuni S, Hahn S, Wagner DD and Karumanchi SA: PAD4 deficiency decreases inflammation and susceptibility to pregnancy loss in a mouse model. Biol Reprod 95: 132, 2016.
8. Rabadi M, Kim M, D'Agati V and Lee HT: Peptidyl arginine deiminase-4-deficient mice are protected against kidney and liver injury after renal ischemia and reperfusion. Am J Physiol Renal Physiol 311: F437-F449, 2016.
9. Rabadi MM, Han SJ, Kim M, D'Agati V and Lee HT: Peptidyl arginine deiminase-4 exacerbates ischemic AKI by finding NEMO. Am J Physiol Renal Physiol 316: F1180-F1190, 2019.
10. Vaughan JE and Walsh SW: Activation of NF-κB in placentas of women with preeclampsia. Hypertens Pregnancy 31: 243-251, 2012.
11. Sakowicz A, Lisowska M, Biesiada L, Płuciennik E, Gach A, Rybak-Krzyszkowska M, Huras H, Sakowicz B, Romanowicz H, Piastowska-Ciesielska AW, *et al*: Placental expression of NEMO protein in normal pregnancy and preeclampsia. Dis Markers 2019: 8418379, 2019.
12. Sakowicz A, Hejduk P, Pietrucha T, Nowakowska M, Płuciennik E, Pospiech K, Gach A, Rybak-Krzyszkowska M, Sakowicz B, Kaminski M, *et al*: Finding NEMO in preeclampsia. Am J Obstet Gynecol 214: 538.e1-538.e7, 2016.
13. Sakowicz A, Pietrucha T, Rybak-Krzyszkowska M, Huras H, Gach A, Sakowicz B, Banaszczyk M, Grzesiak M and Biesiada L: Double hit of NEMO gene in preeclampsia. PLoS One 12: e0180065, 2017.
14. Hu J, Zhang J and Zhu B: Protective effect of metformin on a rat model of lipopolysaccharide-induced preeclampsia. Fundam Clin Pharmacol 33: 649-658, 2019.
15. Graham CH, Hawley TS, Hawley RG, MacDougall JR, Kerbel RS, Khoo N and Lala PK: Establishment and characterization of first trimester human trophoblast cells with extended lifespan. Exp Cell Res 206: 204-211, 1993.
16. Abou-Kheir W, Barrak J, Hadadeh O and Daoud G: HTR-8/SVneo cell line contains a mixed population of cells. Placenta 50: 1-7, 2017.
17. Fan M, Li X, Gao X, Dong L, Xin G, Chen L, Qiu J and Xu Y: LPS induces preeclampsia-like phenotype in rats and HTR8/SVneo cells dysfunction through TLR4/p38 MAPK pathway. Front Physiol 10: 1030, 2019.
18. Livak KJ and Schmittgen TD: Analysis of relative gene expression data using real-time quantitative PCR and the 2(-Delta Delta C(T)) method. Methods 25: 402-408, 2001.
19. Jena MK, Sharma NR, Petitt M, Maulik D and Nayak NR: Pathogenesis of preeclampsia and therapeutic approaches targeting the placenta. Biomolecules 10: 953, 2020.
20. Calicchio R, Buffat C, Vaiman D and Miralles F: Endothelial dysfunction: Role in the maternal syndrome of preeclampsia and long-term consequences for the cardiovascular system. Ann Cardiol Angeiol (Paris) 62: 215-220, 2013 (In French).
21. Pauli JM and Repke JT: Preeclampsia: Short-term and long-term implications. Obstet Gynecol Clin North Am 42: 299-313, 2015.
22. Dai X and Cai Y: Down-regulation of microRNA let-7d inhibits the proliferation and invasion of trophoblast cells in preeclampsia. J Cell Biochem 119: 1141-1151, 2018.
23. Shaw J, Tang Z, Schneider H, Saljé K, Hansson SR and Guller S: Inflammatory processes are specifically enhanced in endothelial cells by placental-derived TNF-α: Implications in preeclampsia (PE). Placenta 43: 1-8, 2016.
24. Harmon AC, Cornelius DC, Amaral LM, Faulkner JL, Cunningham MW Jr, Wallace K and LaMarca B: The role of inflammation in the pathology of preeclampsia. Clin Sci (Lond) 130: 409-419, 2016.
25. Cotechini T, Komisarenko M, Sperou A, Macdonald-Goodfellow S, Adams MA and Graham CH: Inflammation in rat pregnancy inhibits spiral artery remodeling leading to fetal growth restriction and features of preeclampsia. J Exp Med 211: 165-179, 2014.
26. Kadam L, Kilburn B, Baczyk D, Kohan-Ghadr HR, Kingdom J and Drewlo S: Rosiglitazone blocks first trimester in-vitro placental injury caused by NF-κB-mediated inflammation. Sci Rep 9: 2018, 2019.
27. Zaga-Clavellina V, Garcia-Lopez G, Flores-Herrera H, Espejel-Nuñez A, Flores-Pliego A, Soriano-Becerril D, Maida-Claros R, Merchant-Larios H and Vadillo-Ortega F: In vitro secretion profiles of interleukin (IL)-1beta, IL-6, IL-8, IL-10, and TNF alpha after selective infection with Escherichia coli in human fetal membranes. Reprod Biol Endocrinol 5: 46, 2007.
28. Vossenaar ER, Nijenhuis S, Helsen MM, van der Heijden A, Senshu T, van den Berg WB, van Venrooij WJ and Joosten LA: Citrullination of synovial proteins in murine models of rheumatoid arthritis. Arthritis Rheum 48: 2489-2500, 2003.
29. Shelef MA, Sokolove J, Lahey LJ, Wagner CA, Sackmann EK, Warner TF, Wang Y, Beebe DJ, Robinson WH and Huttenlocher A: Peptidylarginine deiminase 4 contributes to tumor necrosis factor α-induced inflammatory arthritis. Arthritis Rheumatol 66: 1482-1491, 2014.
30. Li H, Han SJ, Kim M, Cho A, Choi Y, D'Agati V and Lee HT: Divergent roles for kidney proximal tubule and granulocyte PAD4 in ischemic AKI. Am J Physiol Renal Physiol 314: F809-F819, 2018.
31. Lorquet S, Pequeux C, Munaut C and Foidart JM: Aetiology and physiopathology of preeclampsia and related forms. Acta Clin Belg 65: 237-241, 2010.
32. Martin E, Ray PD, Smeester L, Grace MR, Boggess K and Fry RC: Epigenetics and preeclampsia: Defining functional epimutations in the preeclamptic placenta related to the TGF-β pathway. PLoS One 10: e0141294, 2015.
33. Walker JJ: Pre-eclampsia. Lancet 356: 1260-1265, 2000.
34. Jiang Y, Chen Y and Chen Y: Knockdown of JARID2 inhibits the viability and migration of placenta trophoblast cells in preeclampsia. Mol Med Rep 16: 3594-3599, 2017.
35. Chen D, Yu M, Chen H, Zeng M, Sun Y and Huang Q: Identification and functional characterization of NEMO in Crassostrea gigas reveals its crucial role in the NF-κB activation. Fish Shellfish Immunol 80: 46-55, 2018.
36. Ali Z, Zafar U, Khaliq S and Lone KP: Elevated tumor necrosis factor (TNF)-α mRNA expression correlates with nuclear factor kappa B expression in peripheral blood mononuclear cells in preeclampsia. J Coll Physicians Surg Pak 30: 158-162, 2020.